A New High-Sensitivity Capillary Electrophoresis Detector Cell and Advanced Manufacturing Paradigm

By circumventing laminar flow while expanding the cross section of the analyte, this detector cell greatly increases both the sensitivity and the linearity of capillary electrophoresis. Manufacturing is made feasible by an advanced computer-controlled miniature lathe using machine vision.

by Gary B. Gordon, Richard P. Tella, and Henrique A.S. Martins

Capillary electrophoresis (CE) is a powerful and relatively new analytical technology used to separate and help identify complex aqueous mixtures of chemical and biological samples (see article, page 6). However, CE has often been characterized as a wonderful technology that is scaled too small. This criticism arises from the practical requirement to use very small capillary and sample sizes, which compromises sensitivity. Thus sensitivity is often the most important specification researchers use when comparing CE instruments.

Small Capillaries, Big Headaches

Capillaries for CE are usually 75 micrometers or less in inside diameter. With larger diameters, several adverse factors come into play. First, for a given electrical field, increased diameter means more internal heating in the electrolyte filling the capillary, causing an increased temperature rise. Second, the radial thermal conduction path, by which heat is dissipated, increases in length. As a result, the temperature at the center of the capillary rises even further. This causes a viscosity gradient, which allows molecules of the same species near the center to migrate faster, thus spreading the bands unnecessarily. As a practical compromise, a 50-micrometer inside diameter capillary offers a reasonable balance between sensitivity and resolution.

Sensitivity can be increased somewhat by injecting larger samples. But beyond a point, this practice is undesirable since it degrades resolution and broadens the peaks. For most users, the width of the injection is purposely kept narrow enough so that its contribution to peak broadening is perhaps 10% or less.

The shape of the peak at the detector is characterized by the mathematical convolution of three contributors: the rectangular injection plug, the Gaussian impulse response of the separation capillary, and the shape of the illuminated volume of the detector. Each contributor's spread can be characterized by its variance, a measure of the square of its width. The variance of the detected peak is the sum of the variances of the injection, the capillary, and the detector.

In practice, a typical injection might be one millimeter long and, when spread by diffusion during separation, might produce peaks around 4 mm wide. Such an injection contains only 2 nl of sample, 1000 times less than with liquid chromatography. If the sample contains only one ppm of the constituent of interest, the amount of this constituent that reaches the detector is truly minuscule.

Conventional CE Detectors

CE detectors usually measure UV absorbance. The problem becomes one of efficiently probing or illuminating the band of sample constituent carried in the transparent electrolyte. With 4-mm-wide peaks, a designer might choose to probe a volume of electrolyte 1 mm long to avoid excessive peak broadening.

A second important requirement of detectors is that they be able to quantify peaks accurately, that is, they must be linear.

Fig. 1. Inspiration from a 1903 handbook on glass blowing (from P.N. Hasluck, *Glass Working by Heat and by Abrasion*, Reprinted by Lindsay Publications, 1989; used with permission).

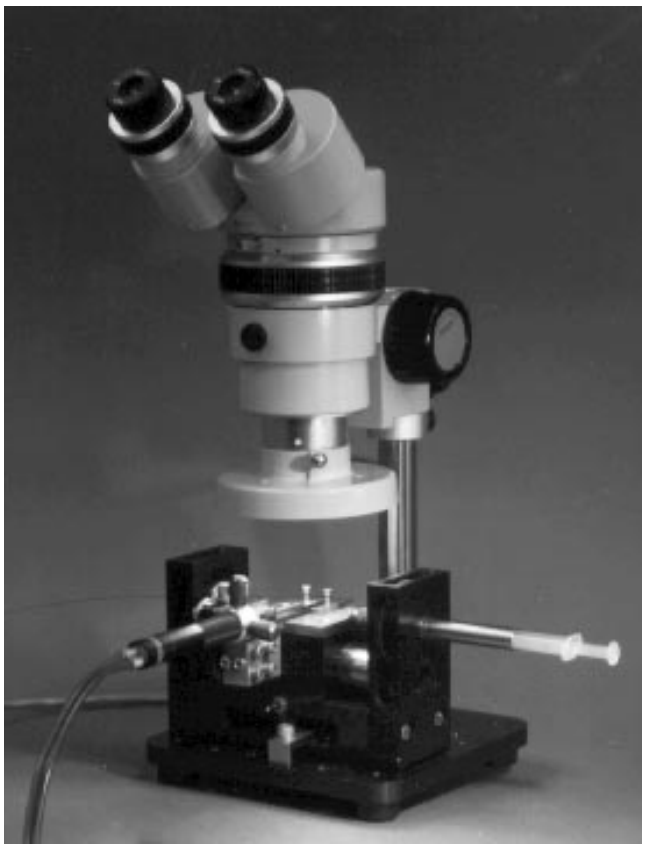

Fig. 2. Manual microglass lathe used for initial prototyping.

To accomplish this, as much of the illumination as possible should pass through the center of the capillary, and especially not travel as stray light around its edges. The intuitive reason for this requirement is that at high absorbencies less light makes it through the analyte, while stray light remains constant and becomes proportionally an increasingly significant contributor. Thus, further decreases in the already weak light passing through the analyte result in less-than-proportional changes in the total light received by the photodiode or spectrophotometer, that is, the detector becomes nonlinear.

Conventional CE detectors attempt to pass illumination radially through the capillary walls, focusing or aperturing the light as well as possible to pass the rays through the center. This configuration is fraught with problems. First, the absorbance path length is so short (the inside diameter of the capillary) that the signal is small and the sensitivity poor. Second, the laws of physical optics prevent most of the deuterium UV excitation lamp's energy from being focused into such a small region, so fewer photons reach the detector and the shot noise increases. Third, it is virtually impossible to prevent stray light from escaping around the capillary inside diameter, so the linearity is poor at high concentrations and quantification is inaccurate.

Lengthening the Path

To obtain a longer absorbance path length, it is tempting to imagine ways of probing the sample volume axially, such as with a Z-shaped cell, since it would better match the long aspect ratio of the bands. The benefit would be a path length of hundreds of micrometers, compared to one 50 micrometers long as in the foregoing example. The path length, however, cannot be the full 1-mm length of the probed volume as might be expected, since the light rays spend most of their time traversing the capillary walls as they zigzag off its periphery. One author briefly considered this option early on but rejected it because of poor linearity, high cost, and modest sensitivity gains.

Given the above difficulties, what other techniques might be used to increase the path length? Would radial expansion to form a bubble be feasible in a capillary not much larger than a human hair? If so, what might be the mixing consequences? These were the starting thoughts for the HP design, influenced by remembrances such as the glassblower sketch, Fig. 1.

To explore the nature of microglassblowing, first a CO_2 laser was tried, with unpleasant results (the capillary pitted and fractured). Next a small battery-powered glass lathe was constructed (Fig. 2.). Commercial pin vises were adapted to form headstock and tailstock clamps, which supported the capillary on both sides of what would become the detector cell. A small syringe, which rotated with the lathe, was used to apply an air pressure of several bar to one end of the capillary. The other end of the capillary was left open and allowed to spin freely. Fused silica softens at a very high temperature (1500°C), but a hobbyist miniature oxyacetylene torch worked very well for applying pinpoint heat. A stereo microscope facilitated watching the bubble growth progress. With this lathe, blowing the bubble cell proved to be relatively easy, despite some dire predictions. In fact, an important component of selling the project was having managers try it themselves.

The Bubble Cell: Laminar Flow, Plug Flow, and Serendipity

The core issue and more interesting science came to play when we began to consider what would be the nature of fluid flow in the cell. The first intuition was that the cell might represent a mixing volume, with either laminar or turbulent flow. With laminar flow, the velocity profile develops a parabolic cross section, with the innermost portion of

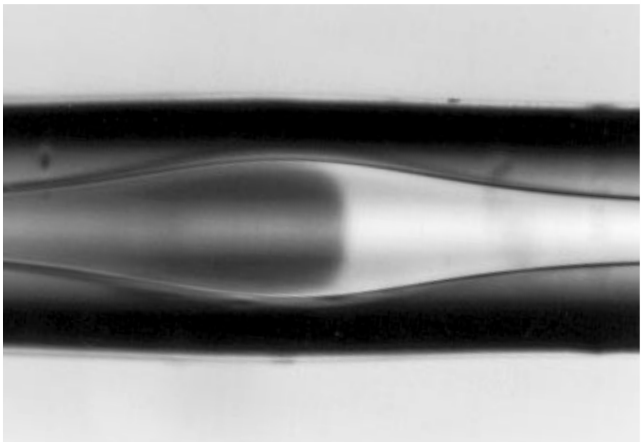

Fig. 3. Microphotograph of the plug flow front, confirming the absence of mixing.

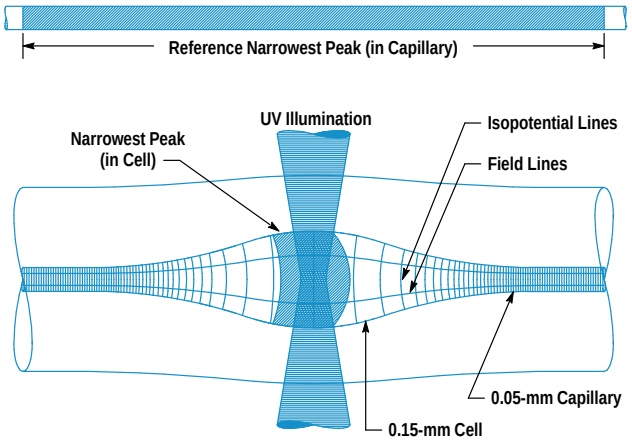

Fig. 4. Electrical field model of the cell.

the stream moving the fastest, and shear smoothly reducing the velocity at the walls to zero. Within this regime mixing and band broadening are considerable. A second and preferred form of flow in the cell is turbulent flow. With this form of flow, the cell can be thought of as a vessel that is repetitively partially refilled, mixed, and then partially re-emptied. With turbulent flow, $(1-1/e)$ or 63% of the volume is swept out with each complete refill. This is the regime used in liquid chromatography detectors, which are, of course, pressure-driven. It is not perfect, because the cell size must be much smaller than desired so as not to broaden the peaks excessively. As a consequence of the small cell size, the detector's sensitivity suffers.

As the project progressed, it became evident that a serendipitous flow balance in the cell might be conceivable. Unlike LC, the CE electrolyte is not driven through the cell by pressure, but rather propelled at its edges by the same electroosmotic forces that drag the electrolyte through the separation capillary. These forces might be reasoned to be less in the cell than in the capillary, just at the same time that the bulk flow requirements in the widening cell would require velocities that were decreasing.

Electroosmotic flow theory teaches that the forces that propel the electrolyte through the capillary act at the thin periphery of the fluid, across a region just micrometers thick, known to electrochemists as the double layer. These forces act to shear this double layer, producing a velocity near the edge that is proportional to force and therefore proportional to the axial electric field. Since the axial field is much lower in the cell because of the greater conductivity of its enlarged cross section, the velocity near the edge of the cell drops dramatically from that in the unexpanded portions of the capillary.

When the electrolyte enters the bubble cell, it encounters a gently increasing cross section. Since the fluid flow is incompressible, the average velocity in the cell drops in inverse proportion to the cross-sectional area. Now, if the velocity at the edge of the cell should also drop in proportion, there would be no tendency for mixing in the cell and the flow would be of the highly desirable plug nature.

This is, in fact, exactly what happens (see Figs. 3 and 4). Both the velocity at the edge of the cell, which drags the contents, and the contents of the cell slow down in exact proportion. This remarkable result means that unlike LC, the flow in the CE bubble cell is of plug nature, without any additional dispersion whatsoever. Thus cells proportionally larger by nearly an order of magnitude than for LC can be used, and much of the sensitivity lost because of the smaller CE apparatus is regained. It is as though the sample plug, long and skinny in the capillary, both slows and transfigures itself into a disc upon entering the cell, thus making possible much higher analysis sensitivity. Subsequently, upon exiting the cell, the plug retakes its original form and speeds along its way.

Fig. 3 shows a photomicrograph of the cell with the front of a separation band passing through it. Although the analyte's constituents continue to separate in the cell as they do in the separation column, the nature of the flow in the cell is dominated by the aforementioned electroosmotic flow.

The cell might, at first, appear to behave simply like a very large capillary and be vulnerable to radial heating, radial density gradients, and counterflow, which cause disastrous band broadening in large capillaries. This is not the case, in part because the the axial power density in the cell is a tiny fraction of the axial power density in the separation portion of the capillary. Further, any counterflow that might tend to develop is small because of the low field and the relatively short time the constituents spend in the cell.

In practice, a typical bubble cell might have a diameter three times that of the capillary within which it is formed. It is then said to have a bubble factor (BF) of three or 3×. In a 3× cell the osmotic velocity is one-ninth that in the separation region of the capillary. Peaks compress in length by a factor of nine, with a 4-millimeter-wide peak shrinking to only 440 micrometers.

How Sensitive?

The sensitivity gain of the bubble cell comes from two contributions: increased signal and less noise. Signals increase in direct proportion to the increase in the length of the absorbance path, which is equal to the bubble factor. We assume that the modern deuterium lamp is itself not a significant source of noise. Rather, the dominant noise derives from the randomness of the photons reaching the detector. Such "shot noise," as it is known, is proportional to the square root of the flux.

As an example of the potential sensitivity gain, consider a 2.5× cell compared to a straight 50-μm capillary. For maximum light flux and minimum stray light, assume that the round source of a deuterium lamp is demagnified and imaged directly onto the analyte. The signal increase is equal to the path length increase, which is equal to the bubble factor, 2.5. To calculate the decrease in noise, it is necessary to know how much the flux increases. Allowing a 10% margin at each side of the cell to minimize stray light effects on linearity, the beam diameter in this example could be increased from 40 μm to 100 μm, or a factor of 2.5. Since the flux increases by the square of the diameter, and the noise drops by the square root of the flux, the noise simply drops by the same bubble factor of 2.5. The signal-to-noise improvement is equal to the product of the path length increase and the noise reduction factor. Since each is

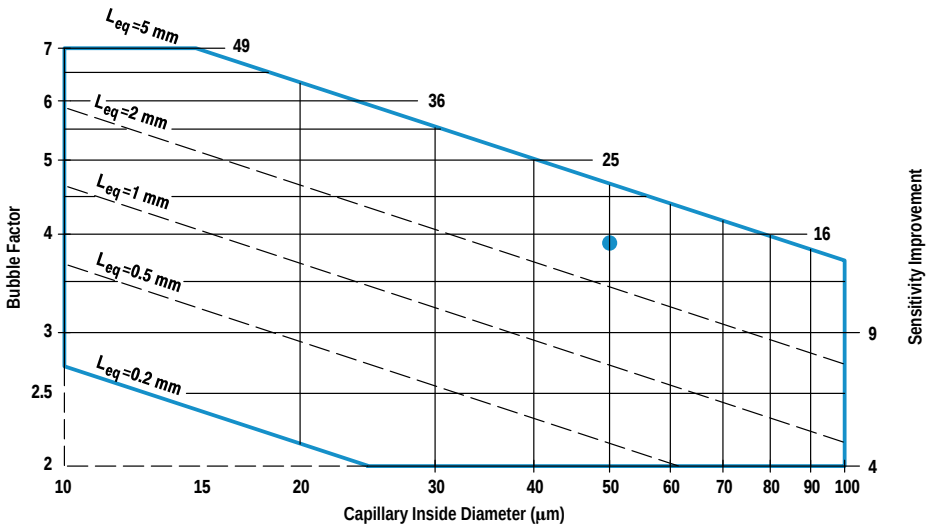

Fig. 5. Nomograph characterizing a bubble cell detector illuminated with a round illumination cone of optimized size and constant intensity. For a given capillary size and equivalent sampled length L_{eq}, an optimum bubble factor is indicated and the sensitivity improvement is predicted. The dot at a capillary diameter of 50 µm and L_{eq} = 3 mm indicates parameters commonly used in the CE literature to compare high-sensitivity detectors.

itself equal to the bubble factor, the signal-to-noise increase, or sensitivity gain, is simply the bubble factor squared, or 6.25× in this example.

Fig. 5 is a nomograph showing to the first order how several parameters are affected when a bubble is added. It assumes imaged illumination as above, but neglects the 10% margins. The dotted lines indicate the size of the sampled volume, as measured by an equivalent length L_{eq} of an analyte plug in the unexpanded capillary. For the above 2.5× cell example, the equivalent sampled length is seen to be 0.8 mm, a length unlikely to contribute noticeable peak broadening. Equivalent sampled lengths larger than roughly a third of the length of the separated peak (caused by too large a bubble) are less desirable because further sensitivity gains are less than proportional and peak broadening will occur. This point is approached with a bubble factor of 3 with 50-µm capillaries and bubble factors of 4 to 6 with small capillaries, using the illumination described.

In practice, demagnifying the source directly onto the cell requires careful and individual alignment. Alternatively, overfilled apertures at the cell can be employed. Since the apertures of the unexpanded and bubble cell capillaries could conceivably be made equal in area, the standard cell and the bubble cell would seem to have the same noise component. Thus the bubble cell would have only the signal boosting advantage, yielding a sensitivity gain identical to the bubble factor. However, common source lamps are not spatially broad enough to image onto and illuminate the full length of the analyte plug in the capillary, but rather only a few tenths of a millimeter of it. Therefore, in practice, bubble cells even in this case offer some noise reduction as well as increased signal. The aperturing practice in general extracts a slight overall noise penalty by limiting the total flux reaching the detector to only those nearly parallel rays that actually traverse the cell.

Reference 1 compares numerous other sensitivity-enhancing paradigms, and as of 1993 cites 42 other references in this burgeoning field. Many of the high-sensitivity detectors it cites are compared at sample volumes of 50-µm diameter and 3-mm length, a point marked on the nomograph with a dot. A bubble cell with comparable volume is seen to have a bubble factor of approximately four and yield a sensitivity enhancement of 15×. Further improvements are possible with cells oval or hourglass-shaped in cross section.

Bubble cells are amenable to use with rectangular capillaries,[2,3,4] fluorescence detection, laser excitation, and spectrographic detection. Reference 5 explores the flow characteristics of bubble cells.

The bubble cell has been characterized here in one of its best configurations, whereas in practice the realized gains depend on the individual optical configuration. For example, the HP G1600A CE instrument adds several important capabilities: spectrographic detection, interchangeability between bubble and conventional detector cells, and apertured self-aligning drop-in cassettes (see article, page 20). HP conservatively represents the cell sensitivity enhancement as being equal to the bubble factor (for example, a 3× bubble increases the sensitivity threefold). Currently HP offers 25-µm capillaries with 5× cells, 50-µm capillaries with 3× cells, and 75-µm capillaries with 3× cells.

The bubble cell affords an easy and economical method to increase the sensitivity of CE. It also increases the linearity and dynamic range of CE, bringing it up to the quantification accuracy enjoyed by liquid chromatography users. Marginal sensitivity and poor linearity are no longer barriers to adopting CE as a powerful new analysis paradigm.

Decision to Automate

HP's original plan was to employ skilled operators to fabricate bubble cell capillaries on manually operated glass lathes of the kind described above. However, the control of dimensional tolerances for diverse bubble sizes, blown in capillaries of different diameters, was recognized as a substantial challenge, especially as production demand increased.

Fortunately, the original work took place in HP Laboratories, HP's central research facility. The climate of HP Laboratories encourages crossfunctional awareness of the diverse technical programs. As a consequence, the prospects of automating the bubble-blowing operation stimulated the interest of the manufacturing research assembly technology team (ATT). The ATT is chartered to explore and create flexible state-of-the-art assembly technology to solve critical, technically challenging, manufacturing problems.

An extended partnership was quickly formed, involving the ATT, the Analytical/Medical Laboratory, which pioneered the bubble cell detector, and HP's Waldbronn Analytical Division, which had product design and manufacturing responsibility.

Drawing heavily on previously created technology, the ATT carried the project from inception to manufacturing production in six months, with the investment of one engineer-year of effort. The remainder of this section describes BubbleWorld, the technical solution, and in particular the crucial role played by computer vision.

As a starting point, given the proven capability of the manual lathe, the ATT determined to leverage its basic configuration. The ATT has many years of application experience employing computer vision as a prime sensory modality for feedback control of robotic assembly systems. It was, therefore, natural to choose computer vision as the vehicle for real-time process monitoring and control and for postfabrication inspection and dimensional characterization.

Specifications and Goals

Specifications and goals were established as follows:

- Capillary initial inside diameter: 25 to 75 μm
- Customizable bubbles: Variable bubble sizes and shapes
  Programmable axial stretch
- Polyimide coating stripping: Flame removal
- Bubble factor: 1× to 5×
- Postinflation axial stretch: 0 to 100 μm
- Reproducibility: ±5 μm on the inflated inside diameter
- Throughput: 2 units/minute
- Hands-off operation, except for loading and unloading
- Automatic quantitative process characterization and logging.

BubbleWorld Hardware

A close-up view of the business section of the microlathe in operation is shown on the cover of this issue, while Fig. 6 illustrates an overall engineering drawing. All of the lathe operations with the exception of capillary loading are under autonomous computer control.

The lathe consists of a fixed headstock and an axially positionable tailstock. The tailstock rides on a preloaded cross-roller assembly, and is positioned by one of four dc servo motors through a cam-link arrangement. This configuration facilitates adjustment to achieve a variety of positional resolutions and ranges, in addition to providing the requisite time response. Similar mechanisms are used to position the radial and axial stages for the torch. A fourth motor drives the spindle.

Identical head and tail spindles are driven by geared belts off a common jack shaft coupled directly to the spindle motor. The capillary is held concentrically in the spindles by two identical collets. Each collet has four fingers formed integrally with the spindle shaft. Collet design was complicated

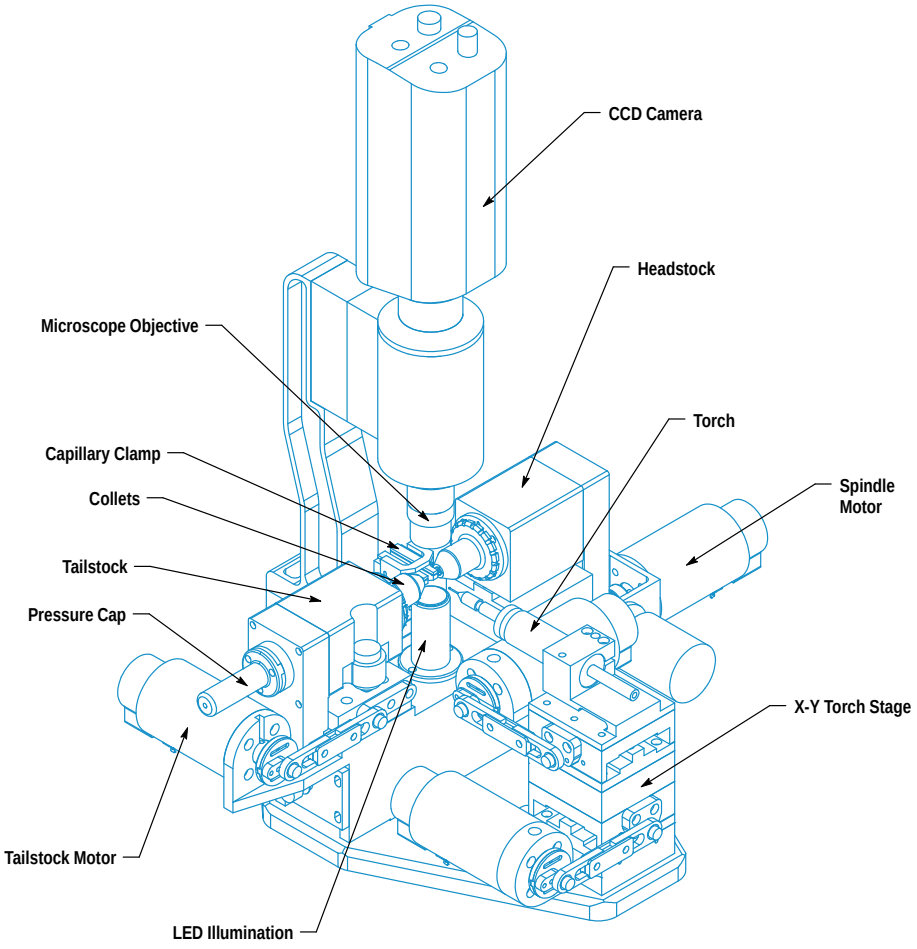

Fig. 6. Schematic drawing of the tabletop-size custom microglass lathe, nicknamed BubbleWorld, which incorporates four servoed axes and machine vision.

by the requirement for clearance to accommodate a stop-bead premounted on the capillary to reference the axial position of the bubble when installing the capillary in the CE. The stop-bead is located close to the bubble, just 4 mm from the collet finger tips, posing a headstock design challenge.

Each collet is actuated to capture the capillary by an outer cap that screws onto the spindle, imparting a radial closing action. A set of locking cylinders set into the stocks actuates to engage the outer cap to inhibit rotation. Proper sequencing of the lock cylinder actuators relative to spindle rotation enables automatic capture and release of the capillary.

Capillaries are inserted through the headstock into the tailstock. Insertion is arrested by the premounted reference stop-bead coming to rest against a registration lip in the headstock collet. The capillary is pressurized through a pressure cap in the headstock, 15 centimeters from where the bubble is to be blown. Since the capillary is one meter long and its flow impedance is large compared to that of the pressure delivery system, the opposite end of the capillary is left open to the atmosphere.

Coaxial alignment of the headstock and tailstock axes is critical to the fabrication of straight capillaries. Alignment is augmented by a small V-grooved finger configuration mounted between the collets. The fingers provide added support to the capillary during bubble blowing.

A miniature hydrogen torch is used, first to burn the polyimide coating before the bubble is blown, and then to heat the capillary during the blowing operation. The torch is mounted on a two-axis stage driven by servo motors and linkage arrangements similar to that used for the tailstock. Because the torch temperature is fixed during operation, the rate of thermal transfer to the capillary is controlled by a programmable radial positioning of the torch.

Proper distribution of heat along the capillary is achieved through programmable velocity control of the axial stage of the torch. This is generally achieved by a dithering motion of controllable amplitude and frequency. The vertical height of the torch is adjustable, but fixed.

A CCD camera fitted with a microscope objective views the capillary from above. High-contrast images of the inner diameter of the capillary are critical for measuring and tracking the bubble growth during blowing. A single diffused LED positioned behind the capillary provides high-contrast images of the inner and outer diameters. An infrared filter suppresses luminous glow from the hydrogen flame and heated capillary.

The workcell controller is an HP Series 9000 Model 720 computer. It runs the HP-UX* operating system and the X11 Window System, and performs all of the data processing, including real-time processing of the bubble images. The computer is equipped with a RasterOps VideoLive EISA-based I/O card used as an image frame grabber for the Cohu CCD camera, and to provide live image observation of the bubble-blowing operation. All motion control is achieved by a Galil four-axis motion controller commanded by the workstation through a serial line. All system sensors and actuators are accessed via the Galil controller as well.

Operation

Bubbles of customizable shape and size can be blown. The process development engineer can create and store numerous bubble-blowing recipes, each containing approximately 30 programmable parameters. Parameters define bubble profile, torch dithering, spin rates, image parameters, and the like. The lathe operator need only select a recipe.

Capillary loading is semiautomatic. The operator inserts the capillary into the open end of the headstock spindle (right side of Fig. 6) until the stop-bead is arrested by the registration lip inside the collet. The operator gently holds the capillary against the lip, while the machine locks the headstock cap and torques the spindle to tighten the collet. The tailstock collet is then similarly tightened. Once both collets are clamped, the supporting fingers are actuated, the synchronized collets are set into rotation, and the capillary is pressurized.

The capillaries are manufactured with a thin layer of protective polyimide. This coating is removed from the bubble section before blowing. This is accomplished by an axially dithered burn-off torching of the capillary. Following burn-off, the capillary is imaged to find the inside diameter. (Image processing is explained below.) The torch again approaches the pressurized capillary to heat it, and expansion commences. During expansion, the bubble image is tracked at approximately 10 frames per second. The output of the tracking operation is processed to support feedback control of the inflation.

If the torch were held at a fixed position during blowing, wall thinning at constant gas pressure would soon precipitate uncontrolled bubble growth. This would stress the ability of the system to control the final bubble size. Instead, in BubbleWorld, when the bubble achieves 80 percent of the goal, bubble growth is slowed by partially withdrawing the torch, allowing a controlled approach to the final diameter.

As an optional final forming option to allow additional control over the shape, the bubble can be axially stretched under program control by displacing the tailstock. Following bubble fabrication, its shape is thoroughly and accurately characterized. Lastly the capillary is removed by reversing the loading sequence. The entire cycle takes about 20 seconds.

Graphical User Interface

Control of the workcell is achieved via a graphical user interface (GUI) built upon a generic GUI developed at HP Laboratories for robotic workcell control.[6] The BubbleWorld GUI consists of a set of X11 windows, each dedicated to a particular task. The operator, the manufacturing engineer, and the maintenance engineer each access different GUIs. A representative set of GUI windows is shown in Fig. 7.

The top-level operator's interface consists of three windows: vision, statistics, and control. The vision window allows the operator to monitor the blowing operation, and includes graphical overlays representing vision system tracking of bubble growth. The statistics window reports bubble-blowing

performance history. The control window presents the operator with a list of predefined process recipes from which to choose.

At a second, password-protected, and more powerful level of control, production engineers can interact with the system to develop processes. This engineer's interface has several windows that allow control of the hardware. It includes a joystick window which allows independent control of each of the axes of the lathe and the torch XY stage. The engineer can control position, speed, and acceleration and the execution of bubble-blowing subtasks such as resetting the workcell, chucking and unchucking the capillary, and burning the polyimide coating. An output window allows the turning on and off of digital output bits and the setting of analog output channel values. An input window portrays the states of several digital input bits and analog channels. A communications window shows the commands sent to the Galil controller and can be used to send debug commands. A database window allows the engineer to store all pertinent parameters for a given recipe, including hardware parameters, and software parameters controlling the vision algorithms that track and measure bubble growth. A vision window accesses vision tracking and measuring parameters. Collectively, these various windows allow easy and intuitive interaction with the workcell, along with appropriate levels of security.

Computer Vision

As previously noted, computer imaging is used for feedback control of the bubble-blowing process and for postprocessing characterization of each bubble. The bubble image is fed from the microscope camera to an image frame grabber board which buffers the image for subsequent processing by the workstation. All image processing is performed by image processing software running on the workstation. We now describe the three vision operations FIND, TRACK, and MEASURE.

The FIND Operation. The purpose of FIND is to construct a matched filter to be used in the subsequent TRACK operation which monitors the evolving profile of the inner wall of the capillary as the bubble is blown. Fig. 8a shows an image of the backlit capillary after the polyimide has been burned away.

The first step in the FIND operation is to high-pass filter the image of the burned-off capillary. This step highlights cross-sectional dark-to-light transitions, as illustrated in Fig. 8b. Local maxima are referenced to a database of edge-pattern sequencing and diametral information. The result is the identification of the capillary walls in the image, as indicated in Fig. 8c.

From the high-pass filter data, a wall-tracking-filter matched to the dimensions of the particular capillary is automatically constructed. The FIND operation is designed to tolerate a degree of spatial noise such as that evident in Fig. 8, as well as noise caused by an exceptionally dusty imaging array.

The TRACK Operation. The TRACK operation tracks the growth of the inner wall of the capillary. The output of this operation is fed back to control the precision blowing of customized bubbles. To support real-time feedback control of bubble-blowing, it is desirable to process bubble images at a rate of at least 10 frames per second. The general-purpose computer is not able to apply TRACK over the entire image at this rate, but neither is this necessary; it suffices to process only a half dozen transverse sections.

The TRACK sequence consists of the following steps. First, the matched filter derived in the FIND operation is used to

Fig. 7. A custom graphical user interface (GUI) was designed to allow the user to develop, execute, and monitor the manufacturing process easily. There are windows for setting up parameters, collecting statistics, and displaying live video of the forming bubble.

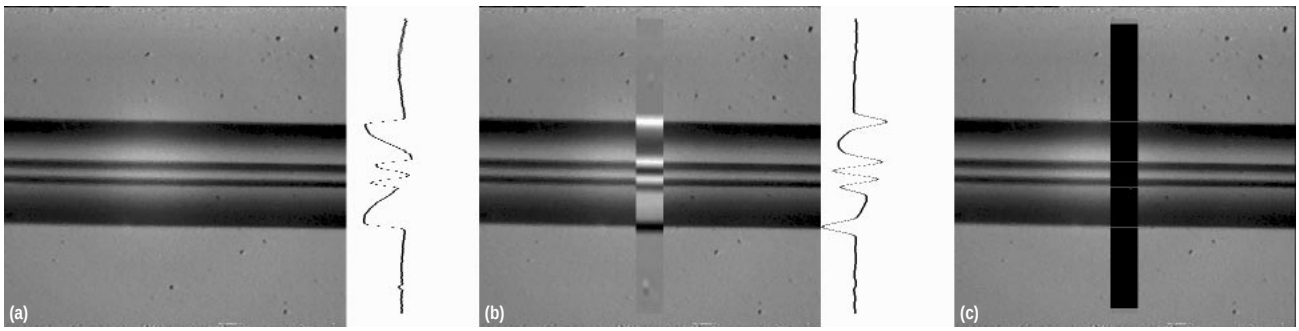

Fig. 8. Machine vision and tracking software are key to automating bubble cell manufacture. (a) The FIND step builds a matched filter to locate the inside diameter of a fresh capillary. (b) A high-pass filter processes a cross section of the capillary image to enhance its edges. (c) Peak detection is used to pinpoint the exact inside diameter.

locate the center of the capillary on both sides of the region where the bubble is to be blown. The central axis of the capillary is then defined by a line connecting these two centerpoints.

The image is then analyzed at several equally spaced transverse segments along the axis of the capillary. At each of these segments, edge and peak detection operations similar to those applied in the FIND operation are performed. The peaks associated with the first dark-to-light transition above and below the central axis define the diameter of the inner wall of the capillary.

In the first few frames, while the capillary is heating up, there will be little expansion. When the greatest inner diameter among the tracked sections achieves a database-specified expansion (typically 120% of the original diameter), the maximum diameter is established by parabolically interpolating through the three cuts corresponding to the largest transverse sections. In subsequent frames, all cuts are equally spaced between the half-maximum expansion points, as shown in Fig. 9.

If, during the TRACK operation, the program establishes that the processed output of any given frame is too noisy, which can be caused by glowing dust particles, polyimide remnants, and the like, then that frame is rejected.

The MEASURE Operation. The last operation, MEASURE, applies the diameter-measuring algorithms described for TRACK, above, to a dense family of sections of the cooled bubble, for the purposes of characterizing the bubble and monitoring the performance of the lathe. Derived information includes the maximum diameter of the bubble and its axial position, and the axial positions of the 90% and 10% expansion sections as illustrated in Fig. 10.

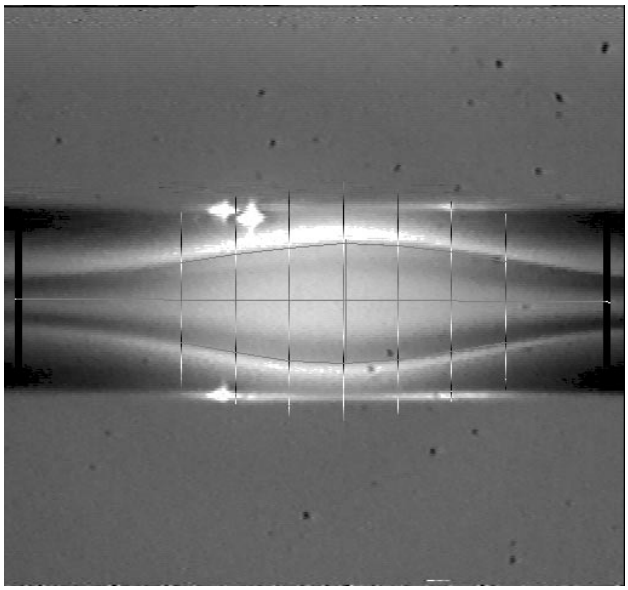

Fig. 9. The TRACK algorithm is used to monitor the capillary inside diameter growth at several axial segments along the forming bubble (the seven vertical lines). Inner edges within each segment of the capillary are tracked in real time. The three largest measurements are fitted with a parabola, the maximum value of which is taken to be the bubble diameter. Cell inflation is progressively arrested as the bubble expands.

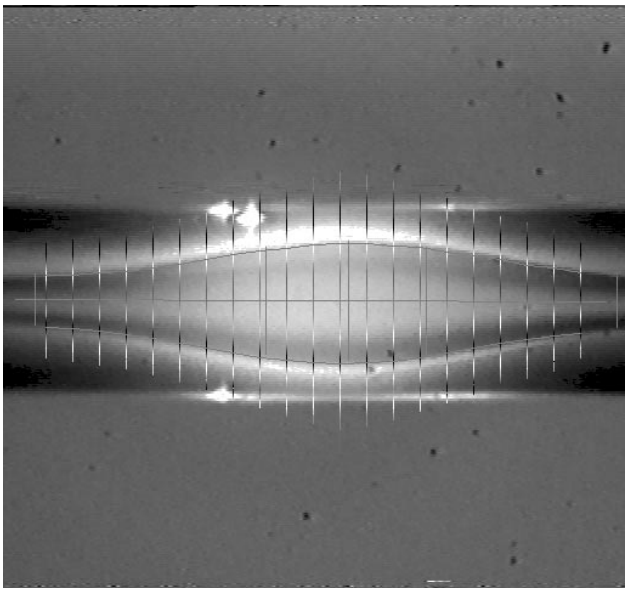

Fig. 10. After blowing is complete, time is less critical and a more complete characterization can be made. The MEASURE operation determines the cell diameter, length, and axial position to an accuracy of 2%.

Conclusion

The geometry of the bubble cell raises capillary electrophoresis to dramatically higher levels of sensitivity and linearity without sacrificing resolution. Application of automation and computer vision to the manufacturing process enables efficient fabrication of consistent, high-quality, customizable, documented bubble cells. Over 40,000 bubble cells have been produced to date.

Acknowledgments

The bubble cell and BubbleWorld efforts were a pleasurable collaboration crossing several organizational and geographical boundaries. The authors are eager to take this opportunity to acknowledge the important contributions of others to the success of this project. During the HP Laboratories EGAD phase (electrophoretic globular absorbance detector), Dick Lacey was responsible for the optics, Jim Young the product design, and Bill Gong the automation electronics. Gratitude is expressed to Barry Willis and Sid Liebes for their continued support, and to Doug McManigill for recognizing the importance of CE to HP. Lastly, special thanks are extended to the Waldbronn Analytical Division's CE business team for so elegantly commercializing this technology.

References

1. M. Albin, Paul D. Grossman, and S.E. Moring, "Sensitivity Enhancement for Capillary Electrophoresis," *Analytical Chemistry*, Vol. 65, no. 10, May 15, 1993, p. 489.

2. *Electrophoresis Capillary with Dispersion-Inhibiting Cross Section*, U.S. Patent #5,324,413 (Gordon), initially filed September 15, 1989.

3. *Rectangular Capillaries for Capillary Electrophoresis*, U.S. Patent #5,092,973 (Zare), filed January 26, 1990.

4. New Product Announcement, R&S Medical, Mountain Lakes, New Jersey.

5. Y. Xue and E.S. Yeung, "Characterization of Band Broadening in Capillary Electrophoresis due to Nonuniform Capillary Geometries," *Analytical Chemistry*, Vol. 66, no. 21, November 1, 1994, pp. 3575-3580.

6. M. Smith, "An Environment for More Easily Programming a Robot," *Proceedings of the IEEE International Conference on Robotics & Automation*, May 1992.

Bibliography

1. *Capillary Zone Electrophoresis Cell System,* U.S. Patent #5,061,361 (Gordon), filed March 6, 1989.

2. G. Gordon, "High-Sensitivity, High-Linearity CE Bubble Cell Detector," poster presentation, *HPCE '91*.